ehp ENVIRONMENTAL HEALTH PERSPECTIVES
http://www.ehponline.org

Comparison of Points of Departure for Health Risk Assessment Based on High-Throughput Screening Data

Salomon Sand, Fred Parham, Christopher J. Portier, Raymond R. Tice, and Daniel Krewski

http://dx.doi.org/10.1289/EHP408

Received: 21 January 2016
Revised: 25 April 2016
Accepted: 13 June 2016
Published: 6 July 2016

Environ Health Perspect DOI: 10.1289/EHP408
Advance Publication: Not Copyedited

Comparison of Points of Departure for Health Risk Assessment Based on High-Throughput Screening Data

Salomon Sand[1,2], Fred Parham[3], Christopher J. Portier[4], Raymond R. Tice[3], and Daniel Krewski[2,5]

[1] Department of Risk Benefit Assessment, National Food Agency, Uppsala, Sweden

[2] McLaughlin Centre for Population Health Risk Assessment, University of Ottawa, Ottawa, Canada

[3] Division of the National Toxicology Program, National Institute of Environmental Health Sciences, Research Triangle Park, North Carolina, USA

[4] Department of Toxicogenomics, Maastricht University, Netherlands

[5] Risk Sciences International, Ottawa, Canada

Address correspondence to: Salomon Sand, National Food Agency, P.O. Box 622, SE-751 26 Uppsala, Sweden. Phone: +46-18-17-5335. E-mail: Salomon.Sand@slv.se.

Running title: Comparison of Points of Departure

Acknowledgments and grant information:

This research was conducted in part while S.S was a Visiting Scientist at the McLaughlin Centre for Population Health Risk Assessment at the University of Ottawa in 2014 and 2015. The work of F.P. and R.T was supported in part by the Intramural Research Program of the National Institutes of Health, National Institute of Environmental Health Sciences. D.K. is employed by the University of Ottawa, and Risk Sciences International, Ottawa, Canada.

Competing financial interests: The authors declare they have not actual or potential competing financial interests.

ABSTRACT

Background: The National Research Council's vision for toxicity testing in the 21st century anticipates that points of departure (PODs) for establishing human exposure guidelines in future risk assessments will increasingly be based on in vitro high-throughput screening (HTS) data.

Objectives: The aim of this study was to compare different PODs for HTS data. Specifically, benchmarks doses (BMDs) were compared to the signal-to-noise crossover dose (SNCD) introduced by Sand et al. (2011) as the lowest dose that may be applicable as a POD.

Methods: Hill models were fit to over 10,000 in vitro concentration-response curves, obtained for over 1,400 chemicals tested as part of the U.S. Tox21 Phase I effort. BMDs and BMDLs corresponding to extra effects (i.e., changes in response relative to the maximum response) of 5, 10, 20, 30, and 40% were estimated for over 8,000 curves, along with BMDs and BMDLs corresponding to additional effects (i.e., absolute changes in response) of 5, 10, 15, 20, and 25%. The SNCD, defined as the dose where the ratio between the additional effect and the difference between the upper and lower bounds of the two-sided 90% confidence interval on absolute effect was 1, 0.67, and 0.5, respectively, was also calculated and compared with the BMDLs.

Results: The $BMDL_{40}$, $BMDL_{25}$, and $BMDL_{18}$, defined in terms of extra effect, corresponded to the $SNCD_{1.0}$, $SNCD0_{.67}$, and $SNCD_{0.5}$, respectively, at the median. Similarly, the $BMDL_{25}$, $BMDL_{17}$, and $BMDL_{13}$, defined in terms of additional effect, corresponded to the $SNCD_{1.0}$, $SNCD0_{.67}$, and $SNCD_{0.5}$, respectively, at the median.

Conclusions: The SNCD may serve as a reference level that guides the determination of standardized BMDs for risk assessment based on HTS concentration-response data. The SNCD may also have potential application as a POD for low-dose extrapolation.

INTRODUCTION

The establishment of health based guidance values is a key outcome of assessing the risk of chemical agents. The determination of such values includes the derivation of a point of departure (POD) from dose-response modeling or, more traditionally, use of the no-observed-adverse-effect-level (NOAEL). Dose-response modeling approaches, specifically the benchmark dose (BMD) method, is generally regarded as the method of choice for derivation of the POD by many international health organizations [Davis et al. 2011; European Food Safety Authority (EFSA) 2009].

For non-genotoxic agents, uncertainty factors accounting for inter- and intra-species differences are applied to the POD derived from the critical effect observed in animals or humans (Dourson et al. 1996). This results in a health-based guidance value, such as a tolerable daily intake (TDI), an acceptable daily intake (ADI), a reference doses (RfD), or a reference concentrations (RfC). Although the exact formulation of the TDI/ADI (WHO/IPCS 2004) differ to some extent from that for the RfD/RfC (EPA 2013), these quantities are derived in essentially the same manner, and can thus be interpreted similarly. The TDI/ADI/RfD is generally set for dietary exposure, while the RfC is generally set for occupational exposures occurring via inhalation: an extensive discussion on occupational exposure limits can be found in Deveau et al. (2015).

In the case of a genotoxic agent, the U. S. Environmental Protection Agency (EPA) risk assessment guidelines recommend low-dose linear extrapolation when (1) there are data to indicate that the dose-response curve has a linear component below the POD, or (2) as a default for a tumor site where the mode of action is not established (EPA 2005). Linear extrapolation to

low doses permits upper-bound estimates of risk at exposure levels of interest, as well as estimation of *risk-specific doses* associated with specific (upper-bound) risk levels; the typical EPA target range for risk management is a 1/1,000,000 to a 1/10,000 increased lifetime risk (EPA 2005). In contrast, both EFSA and the Joint FAO [Food and Agriculture Organization of the United Nations] / WHO [World Health Organization] Expert Committee on Food Additives (JECFA) have recommended a margin of exposure (MOE) approach rather than low-dose linear extrapolation for compounds that are both genotoxic and carcinogenic. EFSA and the JECFA considered that the MOE had the potential to help risk managers to distinguish between large, intermediate, and low health concerns, and thus provide guidance for setting priorities for risk management actions (Barlow et al. 2006). The MOE is also cited in the EPA guidelines, but is positioned as a quantity that provides an indication of the extent of extrapolation of risk estimates from the observed data to the exposure levels of interest in practice (EPA 2005).

Traditional approaches to risk assessment, including the establishment of health based guidance values based on the results of mammalian toxicology tests, have been challenged by the U.S. National Research Council (NRC) in its report, *Toxicity Testing in the 21st Century: A Vision and a Strategy* (NRC 2007) This report envisions that future toxicity tests will be conducted largely in human cells or cell lines in vitro by evaluating cellular responses in a suite of toxicity pathway assays using high-throughput tests. Risk assessments would be performed based on results of such tests, and the equivalents of today's health based guidance values would aim, according to the NRC, at representing dose levels that avoid significant perturbations of the toxicity pathways in exposed human populations. In vitro to in vivo extrapolations would rely on pharmacokinetic models to predict human blood and tissue concentrations under specific

exposure conditions (Andersen and Krewski 2009; Krewski et al. 2009, 2011; NCR 2007). The NRC vision for the future of toxicity testing has recently been incorporated into the EPA's framework for the next generation of risk science (Krewski et al. 2014).

In line with this vision, Judson et al. (2011) presented a framework for estimating the human dose at which a chemical significantly alters biological pathways in vivo, making use of in vitro assay data and an in vitro derived pharmacokinetic model, along with information on population variability and uncertainty. Judson et al. (2011) calculated a 'biological pathway altering dose' (BPAD), which they regarded as conceptually analogous to current risk assessment metrics, in that it combines dose-response data with analysis of uncertainty and population variability to arrive at conservative human exposure limits. Further discussion is needed on how a 'biological significant perturbation', and hence the BPAD, or related metric, should be defined. At a general level, in response to NCR (2007), Crump et al. (2010) considered four possible definitions that were all regarded to incorporate the notion of an exposure threshold for apical response. At a more detailed level, this problem formulation may also concern the technical definition of the POD from a statistical standpoint, which is the focus of the present paper.

Historically, several approaches have been presented in the scientific literature on how to define the BMD and its lower confidence limit (BMDL) (Crump 1984; Murrell et al. 1998; Sand et al. 2006, 2008, 2011; Slob and Pieters, 1998). In their opinion on the BMD, EFSA recommended a default setting for implementation of the BMD approach: in the case of quantal data they recommended that the BMD by default is defined as the dose corresponding to an extra risk of 10%, and for continuous (experimental) data they recommended that BMD by default is defined

as corresponding to a 5% change in response relative to the mean background response (EFSA 2009). The guidance provided by the EPA is similar to that issued by EFSA for quantal data, but the default approaches for continuous data differ between the two agencies (Davis et al. 2011).

Sand et al. (2011) introduced the concept of the signal-to-noise crossover dose (SNCD) as an objective approach to determine the lowest dose applicable as a POD, such that its corresponding effect is not overwhelmed by biological noise or uncertainty in the data. Specifically, the SNCD is defined as the dose where the ratio between the additional effect (the "signal") and the difference between the upper and lower bounds of the two-sided 90% confidence interval on absolute effect (the "noise") correspond to some critical value (critical signal-to-noise ratios of 1, 0.67, and 0.5 are used in this study). In Sand et al. (2011), BMDLs and NOAELs were compared to the SNCD, using values derived from fitting concentration-response data from the U.S. National Toxicology Program (NTP) carcinogenesis bioassay database. The NTP cancer studies represent one of the types of toxicity data that is currently used as a basis for risk assessment. Motivated by the anticipated shift towards the use of in vitro rather than whole animal bioassay data as the basis for risk assessment, the present study extends the comparison of different BMDLs with the SNCD to the case of high throughput in vitro screening data. Using the SNCD as a statistical reference point, this study aims to provide insights into how low response levels in general may be associated with BMDs based on HTS data; the role of the SNCD as a starting point for low-dose extrapolation is also discussed. The analysis performed is based on over 10,000 in vitro concentration-response curves generated on over 1400 compounds as part of the U.S. Tox21 Phase I effort (Tice et al. 2013).

MATERIALS AND METHODS

Dose-response data

The Tox21 program (Tice et al. 2013) is a collaboration between U. S. federal health research agencies for the purpose of developing and applying new methods for chemical toxicity testing. Phase I of the Tox21 program tested approximately 2,800 chemicals, half chosen by the National Toxicology Program (NTP) and half chosen by the U.S. Environmental Protection Agency (EPA). The chemicals were tested in over 50 high-throughput screening assays. Data from the Tox21 Phase I assays consist of 14- or 15- point concentration-response curves. Analysis of compound concentration–response data was performed as described (Inglese et al. 2006). Briefly, raw 1536-well plate reads for each titration point were first normalized relative to the assay specific positive control compound (100%) and DMSO-only wells (basal, 0%) on the same 1536-well plate, and then corrected by applying a pattern correction algorithm using the compound-free 1536-well control plates (i.e., DMSO-only plates) at the beginning and end of the compound plate stack.

Data selection

The assays in Phase I of Tox21 include several types of endpoints (Tice et al. 2013). This analysis includes three groups of assays: cytotoxicity assays, nuclear receptor assays, and assays for stress response pathways. Datasets included in this analysis are listed in Table 1. Most of these data are available in the PubChem BioAssay database (Wang et al. 2012). Each dataset represents one run of an assay on one set of chemicals (EPA or NTP chemicals). Some assays were run more than once on the same chemicals, or in different cell lines, or with multiple

endpoints; those are listed as separate datasets in the table. The analysis included 47 nuclear receptor assay datasets, 23 cytotoxicity assay datasets, and 12 stress response assay datasets.

In addition to the concentration and response data, each concentration-response curve has a curve classification, based on the fit of a Hill equation to the curve (Xia et al. 2011, Huang et al. 2011). There have been two slightly different systems of curve classification. When the more recent curve classification (Huang et al. 2011) was available, it was used; otherwise, the classification used was that from the older system (Xia et al. 2011). For this analysis, only curves in classes 1 and 2 ('complete response curve' and 'incomplete curve', respectively) were used, since the other curve classes indicate the lack of a concentration response or show significant activity only at the highest concentration and are therefore problematic for purposes of fitting a sigmoidal (four parameter) model, like the Hill model. Thus, the present work is limited to address POD derivation for concentration-response curves that are fairly well characterized, as in the previous study using this method (Sand et al. 2011). The assays include replicated data for some of the study chemicals. The present analysis in this paper does not take replication into account, i.e., replicates were considered as separate concentration-response curves; however, an extended analysis focusing on NTP duplicates was also performed. The number of concentration-response curves used from each dataset is given in Table 1. The data normalization and curve classification process includes outlier determination. Outlier points, as specified in the data obtained from Tox21, were not included in the fitting of the Hill function to the data.

Dose-response modeling and estimation of PODs

Dose-response modeling was performed using the Hill model fit to the data by maximum likelihood, with a parametric bootstrap approach for obtaining confidence limits on the PODs derived from the fitted model. The 11,240 concentration-response curves included as a starting point in the analysis were modeled using an automated protocol developed in Matlab. The details associated with the model-fitting approach and POD estimation can be found in the Supplemental Material. The quantities described below were estimated for each curve.

- The BMD, with a two-sided 90% confidence interval, corresponding to extra effects of 5, 10, 20, 30, and 40%. The extra effect is defined as a percent change in response relative to the estimated range of response. Subscript "e" is used to denote these BMDs (e.g., BMD_e, $BMDL_e$, BMD_{10e}, $BMDL_{10e}$).
- The BMD, with a two-sided 90% confidence interval, corresponding to additional effects of 5, 10, 15, 20, and 25%. The additional effect is defined as an absolute change in response compared to the estimated background response. Subscript "a" is used to denote these BMDs (e.g., BMD_a, $BMDL_a$, BMD_{10a}, $BMDL_{10a}$).
- The SNCD corresponding to signal-to-noise ratios of 1.0, 2/3, and 0.5, denoted by $SNCD_{1.0}$, $SNCD_{0.67}$, and $SNCD_{0.5}$, respectively. The point estimate, as well as the upper 95^{th} confidence bound, for the effect (under both the additional and extra effect definitions) at concentrations corresponding to each of the three SNCDs was also derived.

The three types of POD approaches (BMD_e, BMD_a, and SNCD) are illustrated in Figure 1. Also, a discussion of the BMD and SNCD definitions, including why the applied BMD definitions

were preferred over the definition suggested for continuous data by EFSA (2009), is provided in the Supplemental Material.

Comparison of PODs

BMDLs were compared to the SNCD (specifically, $SNCD_{1.0}$, $SNCD_{0.67}$, and $SNCD_{0.5}$). These comparisons were based on curves for which all estimated BMDs and SNCDs (in total, ten BMDs and three SNCDs) were within the experimental concentration range (n = 8,961). Also, results associated with non-significant concentration-response curves (n = 192) and curves for which the estimated maximum response was larger than 150 or smaller than -150 (n = 313 additional curves) were excluded. These combined criteria reduced the 11,240 curves by 25% to 8,456 curves for inclusion in the present study. As noted previously, details of the model-fitting approach and POD estimation can be found in the Supplemental Material.

RESULTS

BMDLs based on extra effect vs. the SNCD

Considering all curves selected for inclusion (n = 8,456), the $BMDL_{40e}$ calibrates to the $SNCD_{1.0}$ at the median (Figure 2A). A concentration between the $BMDL_{20e}$ and the $BMDL_{30e}$ corresponds to the $SNCD_{1.0}$ for stress response assays; the $BMDL_{30e}$ calibrates to the $SNCD_{1.0}$ for cytotoxicity assays; and all BMDLs are below the $SNCD_{1.0}$ at the median for nuclear receptor assays (Figure 2A).

A concentration level between the $BMDL_{20e}$ and the $BMDL_{30e}$ corresponds to the $SNCD_{0.67}$, at the median, across all n = 8,456 curves (Figure 2B). A concentration between the $BMDL_{10e}$ and the $BMDL_{20e}$ corresponds to the $SNCD_{0.67}$ for stress response assays; the $BMDL_{20e}$ calibrates to the $SNCD_{0.67}$ for cytotoxicity assays; and a concentration between the $BMDL_{30e}$ and the $BMDL_{40e}$ corresponds to the $SNCD_{0.67}$ for nuclear receptor assays (Figure 2B). Histograms for the ratios BMDL:$SNCD_{0.67}$ with medians closest to 1 are shown in Figure 3 (considering all n = 8,456 curves).

At the median, the $BMDL_{20e}$ is closest to the $SNCD_{0.5}$ when all 8,456 curves are considered (Figure 2C). The $BMDL_{10e}$ calibrates to the $SNCD_{0.5}$ for stress response assays; the $BMDL_{10e}$ is closest to the $SNCD_{0.5}$ for cytotoxicity assays; and a concentration between the $BMDL_{20e}$ and the $BMDL_{30e}$ corresponds to the $SNCD_{0.5}$ for nuclear receptor assays (Figure 2C).

BMDLs based on additional effect vs. the SNCD

Considering all included curves (n = 8,456), the $BMDL_{25a}$ calibrates to the $SNCD_{1.0}$ at the median (Figure 4A). The $BMDL_{15a}$ calibrates to the $SNCD_{1.0}$ for stress response assays; a concentration between the $BMDL_{20a}$ and the $BMDL_{25a}$ corresponds to the $SNCD_{1.0}$ for cytotoxicity assays; and all BMDLs are below the $SNCD_{1.0}$ at the median for nuclear receptor assays (Figure 4A).

At the median, the $SNCD_{0.67}$ lies between the $BMDL_{15a}$ and the $BMDL_{20a}$ for all curves (n = 8,456) (Figure 4B). The $BMDL_{10a}$ is closest to the $SNCD_{0.67}$ for stress response assays; the $BMDL_{15a}$ calibrates to the $SNCD_{0.67}$ for cytotoxicity assays; and a concentration between the

$BMDL_{20a}$ and the $BMDL_{25a}$ corresponds to the $SNCD_{0.67}$ for nuclear receptor assays (Figure 4B). Histograms for the ratios BMD:$SNCD_{0.67}$ with medians closest to 1 are shown in Figure 5 (considering all n = 8,456 curves).

At the median, the $SNCD_{0.5}$ lies between the $BMDL_{10a}$ and the $BMDL_{15a}$ when all curves (n = 8,456) are considered (Figure 4C). The $BMDL_{05a}$ is closest to the $SNCD_{0.5}$ for stress response assays; the $BMDL_{10}$ approximates to the $SNCD_{0.5}$ for cytotoxicity assays; and a concentration between the $BMDL_{15a}$ and the $BMDL_{20a}$ corresponds to the $SNCD_{0.5}$ for nuclear receptor assays (Figure 4C).

Effect at the SNCD

Figures 6 and 7 show medians, as well as lower 5th and upper 95th percentiles, for the extra and additional effect at the SNCD, respectively, using all included curves (n = 8,456) as the basis. These results indicate that the $SNCD_{1.0}$, $SNCD_{0.67,}$ and $SNCD_{0.5}$ correspond to a median upper bound on the extra effect of 40% (corresponding to the $BMDL_{40e}$), 25% (corresponding to a concentration between $BMDL_{20e}$ and $BMDL_{30e}$), and 18% (corresponding approximately to the $BMDL_{20e}$), respectively (Figure 6). Similar results in Figure 7 show that the $SNCD_{1.0}$, $SNCD_{0.67,}$ and $SNCD_{0.5}$ correspond to a median upper bound of additional effect of 25% (corresponding to the $BMDL_{25a}$), 17% (corresponding to a concentration between the $BMDL_{15a}$ and the $BMDL_{20a}$), and 13% (corresponding to a concentration between the $BMDL_{10a}$ and the $BMDL_{15a}$), respectively. The results illustrated in Figure 6 and 7 are consistent with those presented earlier in Figures 2 - 5.

Analysis of NTP duplicates

Chemicals tested in duplicate on the NTP assay plates were analyzed separately to investigate the stability of estimated quantities across duplicates, as well as the result of merging duplicates. Considering curves in classes 1 and 2 ('complete response curve' and 'incomplete curve', respectively), which the overall analysis is based on, 320 duplicates were identified (i.e., 640 individual curves). At the median, the BMDL differs between these duplicates by a factor 1.6 to 2.2 for BMDLs defined in terms of extra effect, and a factor 1.6 - 2.0 for BMDLs defined in terms of additional effect: the differences decreases with increasing BMR (Table 2). At the median, the SNCD differs between duplicates by a factor of 1.7 - 1.8, depending on the SNR (Table 2). It may be noted that the upper 95th percentile of the BMDL ratio across duplicates is very high at low BMRs, ranging between 100 and 600, depending on the BMR. For other BMDLs, the upper 95th percentile of the ratio of difference between duplicates is in the range of 20 to 40-fold for BMDLs defined in terms of extra effect, and 30 to 50-fold for BMDLs defined in terms of additional effect. For the SNCD, the upper 95th percentile of the ratio of difference between duplicates is in the range of 30-fold.

Table 2 also provides summary information for the ratio between the geometric mean of the SNCD from separate analysis of duplicates, and the SNCD associated with analysis of merged duplicates. At the median this ratio is around 1; for about 60% of the cases the ratio is greater than 1 (Table 2). Overall, the SNCD associated with the analysis of merged duplicates approximates well to the geometric mean of SNCDs from separate analysis of duplicates.

In the Supplemental Material, Section 3 it is shown that summary results describing the effect at the SNCD for the case of separate analysis of duplicates are very similar to the corresponding results associated with the analysis of merged duplicates, and median values for the effect at the SNCD are also similar to those obtained for the whole database (Table S1 vs. Figures 6 and 7).

DISCUSSION

In this article, we compared two points of departure - the traditional BMDL and the recently proposed SNCD - applied to over 8,000 high-throughput experimental concentration-response curves generated during Tox21 Phase I (Tice et al. 2013). Results from these comparisons showed that the $BMDL_{40}$, $BMDL_{25,}$ and $BMDL_{18}$, defined in terms of extra effect, correspond to the $SNCD_{1.0}$, $SNCD_{0.67}$, and $SNCD_{0.5}$, respectively, at the median (Figure 6). Similarly, the $BMDL_{25}$, $BMDL_{17}$, and $BMDL_{13}$, defined in terms of additional effect, correspond to the $SNCD_{1.0}$, $SNCD_{0.67}$, and $SNCD_{0.5}$, respectively, at the median (Figure 7).

Separate analysis of NTP duplicates showed that the difference in BMDLs and SNCDs between duplicates was generally within a factor 2 at the median (Table 2). However, the difference between duplicates was large for a portion of the curves, particularly for BMDLs corresponding to low BMRs (see the upper 95^{th} percentile of the difference between duplicates in Table 2). As shown in Sand et al. (2011), the SNCD decreases with increasing sample size, as larger sample size permit the detection of smaller and smaller effects. This was, however, not observed in the analysis of the NTP duplicates, possibly because the increase in sample size obtained by merging duplicates was too small (a factor of only 2). The dependence of the SNCD or the BMDL on sample size is typically evaluated theoretically assuming that no (or only a minimal) effect in the

mean response occurs: the only effect considered is the effect of more or less data for a curve of the same mean response. The analyses in the present paper indicated that the difference between duplicates with respect to the mean response curve appeared to be larger, by a factor in the range of 2, than the change in SNCD that was obtained by merging duplicates: the SNCD based on the analysis of merged duplicates approximated the geometric mean of the SNCD associated with separate analysis of duplicates (Table 2).

The findings in this paper depend on the study designs used in the database, which are comprised of 13-16 concentrations (sometimes less after removal of outliers) with one observation at each concentration level. SNCDs corresponding to three different SNRs (1, 2/3, and 0.5) were considered. How stringent to be with regard to the selection of the critical SNR that defines the SNCD is a point for discussion even though a critical SNR = 1 intuitively may appear most straight-forward ("signal" equals "noise"). However, even using the least stringent criteria (in terms of level of "noise" allowed) corresponding to an SNR of 0.5, BMDLs corresponding to responses in the range of 10% or below appear to be associated with high uncertainty using the SNCD as a reference (Figures 6 - 7). Similarly, in Figure 2 and 4, it can be noted that the $BMDL_{10}$ is generally below the SNCDs at the median. The analysis of NTP duplicates from Tox21 Phase I also indicated that at least these HTS data can be very uncertain with respect to estimation of BMDLs corresponding to BMRs of 10% or below, since such quantities could differ substantially between individual duplicates (Table 2).

For the NTP cancer bioassay data analyzed in Sand et al. (2011), the $BMDL_{18}$ and $BMDL_{7.3,}$ defined in terms of extra risk, corresponded to the $SNCD_{1.0}$ and $SNCD_{0.67}$, respectively, at the

median. The corresponding BMDLs in this study would be the $BMDL_{40}$ and $BMDL_{25}$, based on the extra effect definition of the BMDL. There are several factors that may explain why the SNCD corresponds to higher BMDLs in this study as compared to Sand et al. (2011). First, data used in the present analysis is continuous in nature, complicating a direct comparison between the two studies. Also, a four parameter model was used in this study, whereas three and two parameter Hill models were used by Sand et al. (2011). A higher level of complexity of the four parameter Hill model can be expected to result in wider confidence intervals, which pushes the SNCD upwards. Further, the SNCD is affected by sample size: whereas the NTP curves evaluated in Sand et al. (2011) typically included 200 observations (four dose groups, including the control, with 50 animals per group), the curves in the present analysis typically included only 13-16 observations (based on one observation per concentration). Furthermore, a bootstrap approach was used in this study for confidence interval estimation, whereas the profile likelihood method was used by Sand et al. (2011). In contrast to Sand et al. (2011), the present analysis adjusted the estimate of variance (the likelihood estimator of the variance) to an unbiased estimator (see Supplemental Material, Section 1) in the process of confidence interval estimation. This adjustment increases the variance (sometimes marginal, depending on the sample size), which increases the SNCD. Also, for these reasons, the BMDL:SNCD ratio may potentially be smaller under the applied bootstrap approach compared to the profile likelihood method. Further analysis is needed to investigate the impact of model dependence (with respect to the mean response model) of the results associated with this analysis. The relative large number of concentration levels (generally 13-16) will, however, constrain dose-response models so they may not assume very different shapes (in the observable region of response). Using normalized data will tend to decrease the variance and therefore decrease the SNCD.

As an example of the use of the SNCD in a risk assessment context, Sand et al. (2011) illustrated how an SNCD based exposure guideline based on low-dose linear extrapolation, using the upper bound on extra risk at the SNCD as starting point, might be calculated. The SNCD appears consistent with the definition of a POD given in the EPA (2005) cancer guidelines, which state that a POD "marks the beginning of extrapolation to lower doses". Burgoon and Zacharewski (2008) described a POD in a way that conceptually resembles the SNCD: their POD was defined "as the point at which the upper 95% confidence limit for the vehicle response intersects the lower 95% confidence limit for the treated response based on parametric assumptions".

The description of the SNCD and the illustration of its potential uses given by Sand et al. (2011) are statistical in nature. However, it has also been suggested that a POD derived from dose-response modeling should include a toxicological interpretation. For example, EFSA's opinion on the BMD states that the response (benchmark response, BMR) associated with the BMD should be in the range of the data in order to avoid having to estimate a BMD by extrapolation. EFSA also notes that their default recommendations, which are based on calibration to the NOAEL approach, may be modified based on statistical or toxicological considerations (EFSA, 2009).

Considering both statistical and biological aspects of the POD, Chiu et al. (2012) and Sand et al. (2012a) argued that the SNCD may represent a starting point for low-dose extrapolation when the upper bound on the risk (or effect) at the SNCD is greater than a 'target effect level' (or benchmark response) established based on biological (Chiu et al. 2012; Sand et al. 2012a) or

risk-management (Sand et al. 2012a) considerations. In case the SNCD is below the target effect level, the dose associated with that effect may be directly used as a POD (Chui et al. 2012).

According to the NRC (2007) vision for future of toxicity testing, increasing attention will be redirected towards determining exposure levels that avoid significant perturbations in toxicity pathways. Judson et al. (2011) introduced the concept of biological pathway activating dose (BPAD) and as a starting point for the establishment of the BPAD used the ToxCast^{TM} AC_{50} values (the concentration at 50% of maximum activity) as PODs in their illustration of the BPAD concept. AC_{50} values have also been considered in other analyses of in vitro data (Burgoon and Zacharewisk 2008; Thomas et al. 2012; Wetmore et al. 2012). As an alternative to using the AC_{50}, Sand et al. (2012b) suggested that the dose at which the slope of the S-shaped dose-response curve changes the most per unit log-dose, denoted BMD_T, may serve as a standardized reference point in the low dose-region for in vitro data. The BMD_T/$BMDL_T$, which approximates the BMD_{20}/$BMDL_{20}$ using the extra effect definition under the Hill model, was introduced by Sand et al. (2006), and suggested as a mathematical definition of a dose within a "transition dose range", as discussed by Slikker et al. (2004). Derivation of PODs like the BMD_T but also the EC_{50} requires adequate characterization of the S-shaped concentration-response curve (including the asymptotes).

As noted in materials and methods, only curves in classes 1 and 2 were considered in this works to support modeling of the full s-shaped curve. A consequence is that results from this analysis are limited in this context, and does not address the issue of POD derivation for concentration-response curves that are poorly characterized. To improve nonlinear parameter estimation,

Shockley (2015) concludes that optimal study designs should be developed or that alternative approaches with reliable performance characteristics should be used to describe concentration-response curves; suggestions that address the latter issue have also been proposed (Hsieh et al. 2015).

It may be questioned whether or not derivation of PODs for in vitro data should involve biological, policy, or risk-management considerations regarding the effect level associated with the POD. At this point it is unclear if avoiding "significant perturbations in toxicity pathway" would imply that some (presumably small) changes in response might be allowed with regard to the suite of critical in vitro endpoints that would be needed to be evaluated in a future risk assessment framework (Krewski et al. 2014). While conceptually reasonable, the determination of BMRs representing "non-adverse" response levels, or similar, for various endpoints is a major challenge within the current risk assessment approach, and, if applicable, such may also be the case for in vitro data. Determination of what changes in biological effect parameters are acceptable may be an even more complex issue in the case of endpoints that are not adverse nor the critical effect or its known and immediate precursor. Issues related to this point have also been discussed by Crump et al. (2010) and Sand et al. (2012b).

It is likely that derivation of PODs from in vitro high-throughput screening data will need to rely on standardized approaches, at least as a starting point. Since the use of in vitro data significantly increases the amount of concentration-response data that needs to be processed, use of standardized modeling protocols, including standardized PODs, may be of importance, at least from a practical point of view. Wignall et al. (2014) recently discussed the use of a standardized

protocol for BMD analysis, which was argued to provide a greater transparency and efficiency then current approaches. Their approach was illustrated for traditional animal toxicity data, but the relevance of this type of approach was also discussed to be of particular value in the case of high-throughput in vitro testing (Wignall et al. 2014). Thomas et al. (2013) have also pointed out that more efficient risk assessment approaches are needed due to the fact that the number of chemicals without toxicity reference values combined with the rate of new chemical development is overwhelming the capacity of the traditional risk assessment. Interestingly, the results of their studies of comparing transcriptional BMD values for the most sensitive pathway with BMD values for the noncancer and cancer apical endpoints showed a high degree of correlation, suggesting that (for their studied chemicals) transcriptional perturbation did not occur at significantly lower doses than apical responses (Thomas et al. 2013).

The SNCD may provide a reference level for determining how low a standardized BMD or BMDL, or similar (potency-based) quantity, may be selected. For example, in risk assessment applications where BMDs are derived for several chemicals (for potency comparisons, for example) or endpoints, a default or screening POD may be chosen such that it is generally not below the SNCD. Based on the present analysis, such a screening level may be lower than the commonly used $AC_{50,}$ discussed above, since the AC_{50} (i.e., the $BMDL_{50}$) is higher than all SNCDs, at the median (Figures 6 and 7). Considering the range of SNCDs evaluated, the $BMDL_{20}$ may be more appropriate as a standardized POD in this context (in terms of extra effect, the $BMDL_{20}$ corresponds to a concentration between the $SNCD_{0.5}$ and the $SNCD_{0.67}$ at the median, and in terms additional effect, the $BMDL_{20}$ corresponds to a concentration between $SNCD_{0.67}$ and $SNCD_{1.0}$ at the median) (Figures 6 and 7). As noted previously, BMDLs

associated with BMRs lower than 10% appear generally not to be supported from a statistical point of view using the SNCD as a reference (Figures 6 and 7). BMRs lower than 10% may, however, be supported for individual curves using the SNCD as a reference.

The SNCD concept may also be used as a starting point for low-dose extrapolation in establishing exposure guidelines corresponding to a given target risk (Chui et al. 2012; Sand et al. 2011; 2012a), using empirical models of a linear or non-linear nature. This may also be viewed as the application of a curve specific uncertainty factor to the SNCD, which depends on the risk/effect at the SNCD and the empirical extrapolation model used (Sand et al. 2011). It may be noted that, if the dose-response is sublinear, the risk estimate by the SNCD generally decreases as the sample size increases, as discussed in Sand et al. (2011). Increasing sample size makes the SNCD become lower and under a linear extrapolation approach (by drawing a straight line between the upper bound of risk/effect at the SNCD and the background response), the dose corresponding to a given target risk/effect then becomes higher (less conservative) since the slope of the linear model becomes lower. While this approach may be motivated for severe apical endpoints, it remains to be seen under which circumstances an approach involving low-dose extrapolation would be required in risk assessments based on in vitro data.

CONCLUSION

The NRC vision for the future of toxicity testing suggests that PODs for risk assessments may be increasingly based on in vitro HTS data, a notion that has been incorporated into EPA's framework for the next generation of risk science. The technical definition of a POD derived from dose-response modeling has stimulated significant discussion within the current risk

assessment paradigm: the present study has extended this discussion to the case of HTS data using a large database comprised of HTS experimental concentration-response curves generated during Tox21 Phase I. How the POD for HTS data should be designed to support future risk assessment applications warrants further discussion. While endpoint specific definitions of the BMD, based on judgment applied on a case by case basis, is conceptually appropriate, it may be problematic in practice in light of the vast amount of data that will be generated through the greatly expanded application of robotically mediated high throughput in vitro testing. Such rich data may require the use of standardized procedures and PODs for practical application and meaningful interpretation. The SNCD may provide a reference level that guides the determination of standardized BMDs, or similar potency-based measures, such that they are not subject to excessive uncertainty. Based on the present data base, comprising over 8,000 HTS curves, such a BMD and BMDL may need to be associated with a response higher than standard responses of 5 or 10%. The SNCD may also have potential use as a starting point for low-dose extrapolation in the process of establishing safe exposure limits.

REFERENCES

Andersen ME, Krewski D. 2009. Toxicity testing in the 21st century: bringing the vision to life. Toxicol. Sci. 107:324-30.

Barlow S, Renwick AG, Kleiner J, Bridges JW, Busk L, Dybing E, et al. 2006. Risk assessment of substances that are both genotoxic and carcinogenic report of an international conference organized by EFSA and WHO with support of ILSI Europe. Food Chem Toxicol 44:1636-1650.

Burgoon LD, Zacharewski TR. 2008. Automated quantitative dose-response modeling and point of departure determination for large toxicogenomic and high-throughput screening data sets. Toxicol Sci 104:412-418.

Chiu WA, Guyton KZ, Hogan K, Jinot J. 2012. Approaches to human health risk assessment based on the signal-to-noise crossover dose. Environ Health Perspect 120:A264.

Crump K. 1984. A new method for determining allowable daily intakes. Fundam Appl Toxicol 4:854-871.

Crump K, Chen C, Louis T. 2010. The future use of in vitro data in risk assessment to set human exposure standards - challenging problems and familiar solutions. Environ Health Perspect 118:1350-1354.

Davis JA, Gift JS, Zhao QJ. 2011. Introduction to benchmark dose methods and U.S. EPA's benchmark dose software (BMDS) version 2.1.1. Regul Toxicol Pharmacol 254:181-191.

Deveau M, Chen CP, Johanson G, Krewski D, Maier A, Niven KJ, et al. 2015. The global landscape of occupational exposure limits - implementation of harmonization principles to guide limit selection. J Occup Environ Hyg 12 Suppl 1:S127-144

Dourson M, Felter S, Robinson D. 1996. Evolution of science-based uncertainty factors in noncancer risk assessment. Regul Toxicol Pharmacol 24:108-120.

EFSA (European Food Safety Authority). 2009. Guidance of the Scientific Committee on a request from EFSA on the use of the benchmark dose approach in risk assessment. The EFSA Journal 1150:1-72.

Hsieh J-H, Sedykh A, Huang R, Xia M, Tice RR. 2015. A data analysis pipeline accounting for artifacts in Tox21 quantitative high-throughput screening assays. J Biomol Screen [Epub ahead of print].

Huang R, Xia M, Cho M-H, Sakamuru S, Shinn P, Houck KA, et al. 2011. Chemical genomics profiling of environmental chemical modulation of human nuclear receptors. Environ Health Perspect 119: 1142-1148.

Inglese J, Auld DS, Jadhav A, Johnson RL, Simeonov A, Yasgar A, et al. 2006. Quantitative

high throughput screening: a titration-based approach that efficiently identifies biological activities in large chemical libraries. Proc Natl Acad Sci USA 103:11473-11478.

Judson RS, Kavlock RJ, Setzer RW, Hubal EA, Martin MT, Knudsen TB, et al. 2011. Estimating toxicity-related biological pathway altering doses for high-throughput chemical risk assessment. Chem Res Toxicol 24:451-462.

Krewski D, Andersen ME, Mantus E, Zeise L. 2009. Toxicity testing in the 21st century: implications for human health risk assessment. Risk Anal 29:474-79.

Krewski D, Westphal M, Al-Zoughool M, Croteau MC, Andersen ME. 2011. New directions in toxicity testing. Annu Rev Public Health 32:161-178.

Krewski D, Westphal M, Andersen ME, Paoli G, Chiu W, Al-Zoughool M, et al. 2014. A framework for the next generation of risk science. Environ Health Perspect. 122:796-805.

Murrell JA, Portier CJ, Morris RW. 1998. Characterizing dose-response I: Critical assessment of the benchmark dose concept. Risk Anal 18:13-26.

NCR (National Research Council). 2007. Toxicity testing in the 21st century: A vision and a strategy. Washington, DC: National Academies Press.

Sand S, von Rosen D, Victorin K, Falk Filipsson A. 2006. Identification of a critical dose level for risk assessment: developments in benchmark dose analysis of continuous endpoints. Toxicol Sci 90:241-251.

Sand S, Victorin K, Falk Filipsson A. 2008. The current state of knowledge on the use of the benchmark dose concept in risk assessment. J Appl Toxicol 28:405-421.

Sand S, Portier CJ, Krewski D. 2011. A signal-to-noise crossover dose as the point of departure for health risk assessment. Environ Health Perspect 119:1766-1774.

Sand S, Portier CJ, Krewski D. 2012a. Signal-to-noise crossover dose: Sand et al. respond. Environ Health Perspect 120:A264.

Sand S, Ringblom J, Håkansson H, Öberg M. 2012b. The point of transition on the dose-effect curve as a reference point in the evaluation of in vitro toxicity data. J Appl Toxicol 32:843-849.

Shockley KR. 2015. Quantitative high-throughput screening data analysis: challenges and recent advances. Drug Discovery Today 20(3):296-300.

Slikker W, Andersen ME, Bogdanffy MS, Bus JS, Cohen SD, Conolly RB, et al. 2004. Dose-dependent transitions in mechanisms of toxicity. Toxicol Appl Pharmacol 201:203-225.

Slob W, and Pieters MN. 1998. A probabilistic approach for deriving acceptable human intake limits and human health risks from toxicological studies: general framework. Risk Anal 18:787-798.

Thomas RS, Black MB, Li L, Healy E, Chu TM, Bao W, et al. 2012. A comprehensive statistical analysis of predicting in vivo hazard using high-throughput in vitro screening. Toxicol Sci 128:398-417.

Thomas RS, Wesselkamper SC, Wang NC, Zhao QJ, Petersen DD, Lambert JC, et al. 2013. Temporal concordance between apical and transcriptional points of departure for chemical risk assessment. Toxicol Sci 134:180-194.

Tice RR, Austin CP, Kavlock RJ, Bucher JR. 2013. Improving the human hazard characterization of chemicals: A Tox21 update. Environ Health Perspect 121:756-765.

U.S. EPA (U.S. Enviromental Protection Agency). 2013. U.S. EPA home page: http://www.epa.gov/risk/glossary.html

U.S. Environmental Protection Agency (U.S. EPA). 2005. Guidelines for carcinogen risk assessment. Final report. EPA/630/P-03/001F. Risk Assessment Forum, U.S. Environmental Protection Agency, Washington, DC.

Wang Y, Xiao J, Suzek TO, Zhang J, Wang J, Zhou Z, et al. 2012. PubChem's BioAssay Database. Nucleic Acids Res. 40(1):D400-12.

Wetmore BA, Wambaugh JF, Ferguson SS, Sochaski MA, Rotroff DM, Freeman K, et al. 2012. Integration of dosimetry, exposure and high-throughput screening data in chemical toxicity assessment. Toxicol Sci 125:157-174.

Wignall JA, Shapiro AJ, Wright FA, Woodruff TJ, Chiu WA, Guyton KZ, Rusyn I. 2014. Standardizing benchmark dose calculations to improve science-based decisions in human health assessments. Environ Health Perspect 122:499-505.

WHO/IPCS (World Health Organization, International Programme on Chemical Safety). 2004. Harmonization document no. 1. IPCS risk assessment terminology. World Health Organization, Geneva.

Xia M, Shahane S, Huang R, Titus SA, Shum E, Zhao Y, et al. 2011. Identification of quaternary ammonium compounds as potent inhibitors of hERG potassium channels. Toxicol Appl Pharmacol 252:250-258.

Table 1. Datasets used in the analysis.

Assay	**PubChem BioAssay ID (AID)[a]**	**Chemical Source**	**Number of Concentration-Response Curves in Classes 1 and 2[b]**
Nuclear receptor assays			
Human androgen receptor agonist	588515	EPA	114
Human androgen receptor antagonist	588516	EPA	289
Human estrogen α receptor agonist	588514	EPA	230
Human estrogen α receptor antagonist		EPA	429
Human farnesoid X receptor agonist	588527	EPA	20
Human farnesoid X receptor antagonist	588526	EPA	199
Human glucocorticoid receptor agonist	588532	EPA	15
Human glucocorticoid receptor antagonist	588533	EPA	154
Human peroxisome proliferator-activated receptor γ agonist	588536	EPA	181
Human peroxisome proliferator-activated receptor γ antagonist	588537	EPA	206
Human peroxisome proliferator-activated receptor δ agonist	588534	EPA	106
Human peroxisome proliferator-activated receptor δ antagonist	588535	EPA	159
Human retinoid X receptor agonist	588544	EPA	337
Human retinoid X receptor antagonist	588546	EPA	245
Human thyroid receptor agonist	588545	EPA	41
Human thyroid receptor antagonist	588547	EPA	98
Human vitamin D receptor agonist	588543	EPA	24
Human vitamin D receptor antagonist	588541	EPA	120
Human androgen receptor agonist	588515	NTP	146
Human androgen receptor antagonist	588516	NTP	367
Human aryl hydrocarbon receptor agonist	651777	NTP	86
Human estrogen α receptor agonist	588514	NTP	157
Human estrogen α receptor antagonist	588513	NTP	139
Human farnesoid X receptor agonist	588527	NTP	9
Human farnesoid X receptor antagonist	588526	NTP	211
Human glucocorticoid receptor agonist	588532	NTP	14
Human glucocorticoid receptor antagonist	588533	NTP	189
Human peroxisome proliferator-activated receptor α agonist	651778	NTP	13
Human peroxisome proliferator-activated receptor α antagonist	n/a	NTP	227
Human peroxisome proliferator-activated receptor α antagonist	n/a	NTP	237

Human peroxisome proliferator-activated receptor γ agonist, CHO cells	n/a	NTP	16
Human peroxisome proliferator-activated receptor γ agonist, CHO cells	n/a	NTP	31
Human peroxisome proliferator-activated receptor γ agonist, Hek293 cells	588536	NTP	77
Human peroxisome proliferator-activated receptor γ antagonist, Hek293 cells	588537	NTP	232
Human peroxisome proliferator-activated receptor δ agonist	588534	NTP	110
Human peroxisome proliferator-activated receptor δ antagonist	588535	NTP	245
Human pregnane X receptor agonist	720659	NTP	192
Human retinoid X receptor agonist	588544	NTP	177
Human retinoid X receptor antagonist	588546	NTP	97
Human thyroid receptor agonist	588545	NTP	89
Human thyroid receptor antagonist	588547	NTP	67
Human vitamin D receptor agonist	588543	NTP	16
Human vitamin D receptor antagonist	588541	NTP	94
Rat pregnane X receptor agonist	651751	NTP	153
Cytotoxicity assays			
Viability in 3T3 cells	n/a	NTP	236
Viability in BJ cells	421	NTP	80
Viability in endotoxin assay	n/a	NTP	334
Viability in glucocorticoid receptor assay	n/a	NTP	111
Viability in H-4-II-E cells	543	NTP	231
Viability in Hek293 cells	131	NTP	131
Viability in HeLa cells in the antioxidant response element assay	n/a	NTP	111
Viability in HepG2 cells in the antioxidant response element assay	720653	NTP	62
Viability in HepG2 cells	433	NTP	156
Viability in HepG2 cells	n/a	NTP	189
Viability in HepG2 cells	n/a	NTP	173
Viability in HUVEC cells	542	NTP	110
Viability in Jurkat cells	426	NTP	213
Viability in mesangial cells	546	NTP	108
Viability in mesangial cells	n/a	NTP	51
Viability in MRC-5 cells	434	NTP	73
Viability in N2a cells	540	NTP	202
Viability in nuclear factor κB assay	n/a	NTP	27
Viability in p53 assay	743292	NTP	69
Viability in peroxisome proliferator-activated	n/a	NTP	95

receptor α assay			
Viability in rat renal proximal tubule cells	545	NTP	159
Viability in SH-SY5Y cells	544	NTP	244
Viability in SK-N-SH cells	435	NTP	126
Stress response assays			
Antioxidant response element, beta-lactamase reporter	651741	NTP	583
Antioxidant response element, luciferase reporter	720636	NTP	192
Cyclic AMP response element agonist	n/a	NTP	162
Cyclic AMP response element antagonist	n/a	NTP	139
Endoplasmic reticulum stress response element	n/a	NTP	51
Heat shock protein, luciferase reporter	n/a	NTP	7
Heat shock protein, luciferase reporter	n/a	NTP	31
Heat shock protein, beta-lactamase reporter	n/a	NTP	24
Hypoxia inducible factor 1	2120	NTP	73
Nuclear factor κB agonist	651749	NTP	26
Nuclear factor κB antagonist	n/a	NTP	231
p53 gene	651743	NTP	72

[a] Assays with AID given as 'n/a' are not available on PubChem

[b] Each concentration-response curve has a curve classification, based on the fit of a Hill equation to the curve (Xia et al. 2011, Huang et al. 2011). For this analysis, only curves in classes 1 and 2 ('complete response curve' and 'incomplete curve', respectively) were used, since the other curve classes indicate the lack of a concentration response or show significant activity only at the highest concentration and are therefore problematic for purposes of fitting a sigmoidal (four parameter) model, like the Hill model.

Table 2. Comparison of BMDLs and SNCDs for NTP duplicates.

Type of comparison	**Quantity**	**Median**	**5th percentile**	**95th percentile**	***X*[e]**
BMDL ratio between duplicates (extra effect)[a]	$BMDL_{05e}$	2.2	1.0	625	-
	$BMDL_{10e}$	1.9	1.0	140	-
	$BMDL_{20e}$	1.7	1.0	43	-
	$BMDL_{30e}$	1.6	1.0	26	-
	$BMDL_{40e}$	1.6	1.0	17	-
BMDL ratio between duplicates (additional effect)[b]	$BMDL_{05a}$	2.0	1.0	455	-
	$BMDL_{10a}$	1.7	1.0	104	-
	$BMDL_{15a}$	1.6	1.0	51	-
	$BMDL_{20a}$	1.6	1.0	32	-
	$BMDL_{25a}$	1.6	1.0	29	-
SNCD ratio between duplicates[c]	$SNCD_{1.0}$	1.7	1.0	29	-
	$SNCD_{0.67}$	1.7	1.0	28	-
	$SNCD_{0.5}$	1.8	1.0	35	-
$SNCD_{duplicate\ GM}$: $SNCD_{merged}$[d]	$SNCD_{1.0}$	1.0	0.45	3.1	0.58
	$SNCD_{0.67}$	1.1	0.47	3.0	0.62
	$SNCD_{0.5}$	1.1	0.44	3.1	0.63

Note: the analysis is based on 307 duplicates (614 individual curves). There are in total 320 NTP duplicates with curves in classes 1 and 2; i.e., 320-307 = 13 curves have been excluded from this analysis since they did not show a concentration-response trend according to criteria described in Supplemental Material, Section 1. The BMDL ratios have been calculated so that they are always larger than 1 (max value / min value).

[a] Ratio of extra effect BMDLs between duplicates.

[b] Ratio of additional effect BMDLs between duplicates.

[c] Ratio of SNCDs between duplicates.

[d] Ratio of the geometric mean of the SNCD between duplicates ($SNCD_{duplicate\ GM}$) and the corresponding SNCD resulting from analysis of merged duplicates ($SNCD_{merged)}$.

[e] Fraction of curves for which the ratio is higher than 1.

FIGURE LEGENDS

Figure 1. Illustration of the three types of POD approaches considered in the study. Nuclear receptor assay concentration response data on pimozide is used as an example (solid circles). The Hill model has been fitted to the data - in all three cases the solid curves that describe the mean response is the same, but the two-sided 90% confidence intervals around the mean response (the dotted curves) depend on the POD approach considered. Part A): the BMD associated with a 10% extra effect (BMD_{10e}) is 0.24 units (solid red vertical line), and the lower 5^{th} and upper 95^{th} confidence limits (vertical dotted lines) are 0.15 ($BMDL_{10e}$) and 0.37 units, respectively. Part B): the BMD associated with a 10% additional effect (BMD_{10a}) is 0.28 units (solid red vertical line), and the lower 5^{th} and upper 95^{th} confidence limits (vertical dotted lines) are 0.18 ($BMDL_{10a}$) and 0.42 units, respectively. Part C): the $SNCD_{1.0}$ associated with a signal-to-noise ratio (SNR) of 1.0 is 0.31 units (solid red vertical line). The difference between the lower and upper bound on absolute effect at the SNCD is ≈ 10.4 - (-1.2) = 11.6 (difference between the horizontal dotted lines). Since the SNR is 1.0, this approximates to the point estimate of additional effect at the SNCD which is ≈ 4.6 - (- 7.0) = 11.6 (difference between the horizontal solid line and the background response according to the fitted model). In this example $SNCD_{1.0}$ is about twice the size of the BMDLs.

Figure 2. Ratios of the $BMDL_e$ to the SNCD with BMDLs defined in terms of extra effects of 5, 10, 20, 30, and 40%. Ratios are given in terms of medians (solid circles), and an interval describing the lower 5^{th} and upper 95^{th} percentile, based on different stratifications of the data. Red (large) circles correspond to results based on all selected curves (n = 8,456); blue circles

correspond to results based on cytotoxicity assays (n = 3,130); yellow circles correspond to results based on nuclear receptor assays (n = 4,603); and green circles are results based on stress response assays (n = 723). (A) Ratios of the $BMDL_e$ to the $SNCD_{1.0}$. (B) Ratios of the $BMDL_e$ to the $SNCD_{0.67}$. (C) Ratios of the $BMDL_e$ to the $SNCD_{0.5}$.

Figure 3. Histograms for the ratios $BMDL_e$:$SNCD_{0.67}$ (BMDLs are based on extra effect) with medians closest to 1 based on all included curves (n = 8,456).

Figure 4. Ratios of the $BMDL_a$ to the SNCD with BMDLs defined in terms of additional effects of 5, 10, 15, 20, and 25%. Ratios are given in terms of medians (solid circles), and an interval describing the lower 5^{th} and upper 95^{th} percentile, based on different stratifications of the data. Red (large) circles correspond to results based on all selected curves (n = 8,456); blue circles correspond to results based on cytotoxicity assays (n = 3,130); yellow circles correspond to results based on nuclear receptor assays (n = 4,603); and green circles are results based on stress response assays (n = 723). (A) Ratios of the $BMDL_a$ to the $SNCD_{1.0}$. (B) Ratios of the $BMDL_a$ to the $SNCD_{0.67}$. (C) Ratios of the $BMDL_a$ to the $SNCD_{0.5}$.

Figure 5. Histograms of the ratios $BMDL_a$:$SNCD_{0.67}$ (BMDLs are based on additional effect) with medians closest to 1 based on all included curves (n = 8,456).

Figure 6. Extra effect at the SNCD. Medians (solid circles) and an interval describing the lower 5^{th} and upper 95^{th} percentile are shown based on all included curves (n = 8,456). Red circles

correspond to the upper bound of effect, and green circles correspond to the point estimate of effect.

Figure 7. Additional effect at the SNCD. Medians (solid circles) and an interval describing the lower 5th and upper 95th percentile are based on all included curves (n = 8,456). Red circles correspond to the upper bound of effect, and green circles correspond to the point estimate of effect.

Figure 1a.

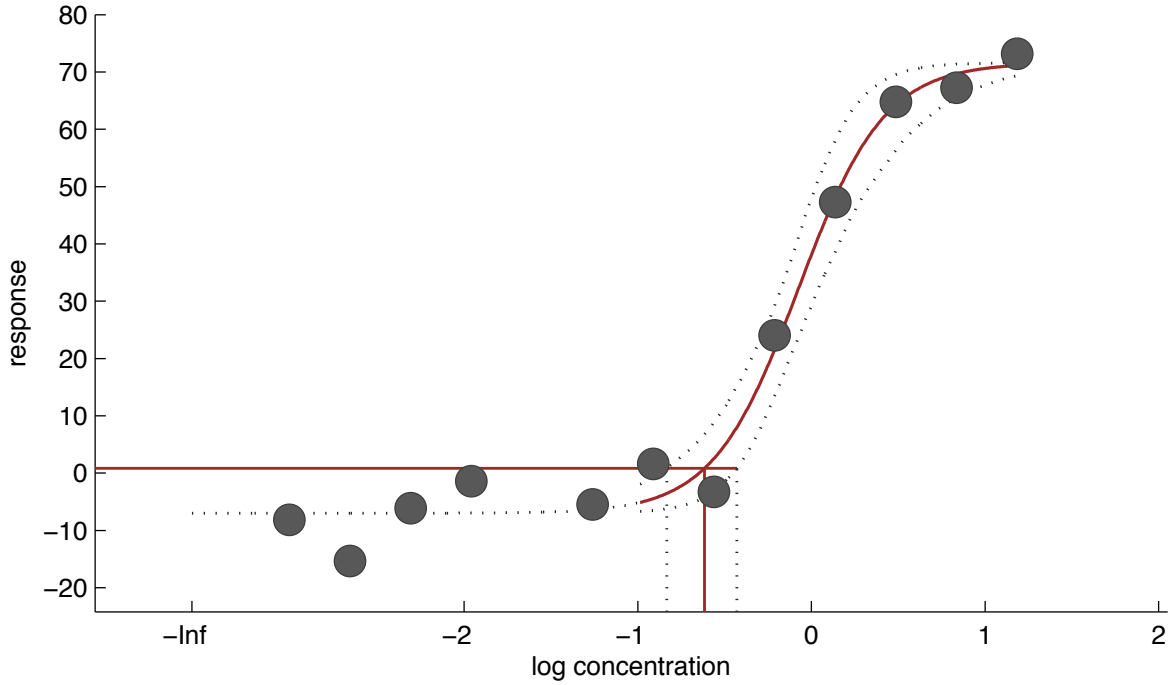
80
70
60
50
40
30
20
10
0
−10
−20
response
−Inf
−2
−1
0
1
2
log concentration

Figure 1b.

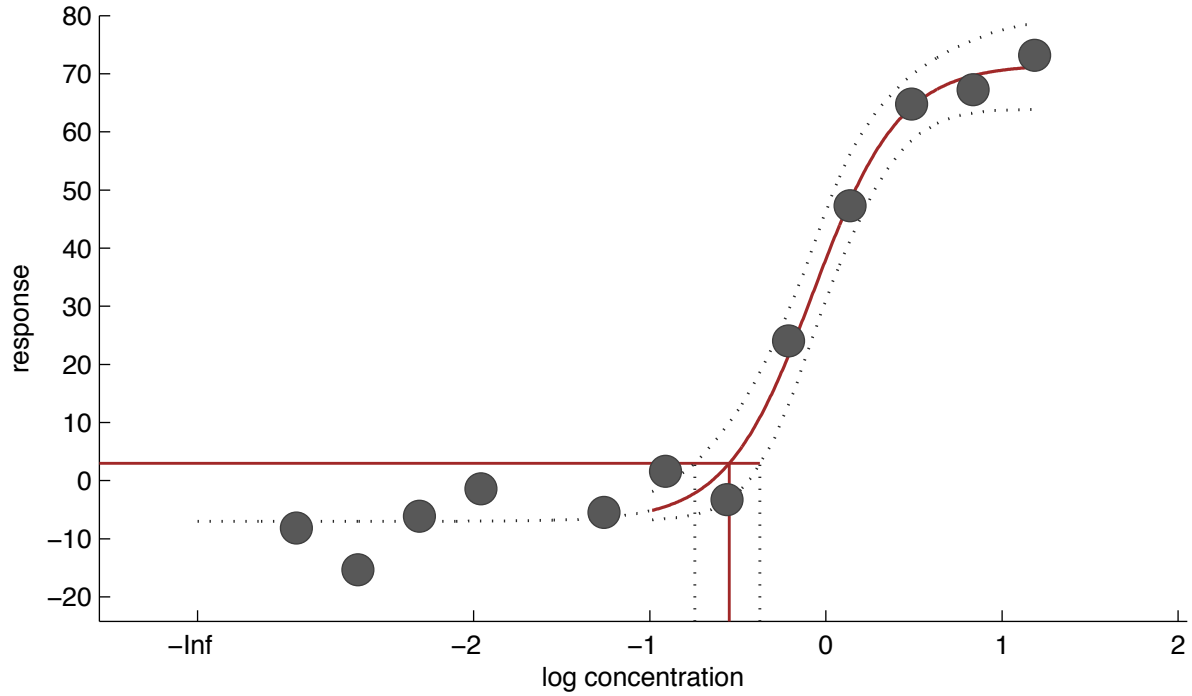
80
70
60
50
40
30
20
10
0
−10
−20
response
−Inf
−2
−1
0
1
2
log concentration

Figure 1c.

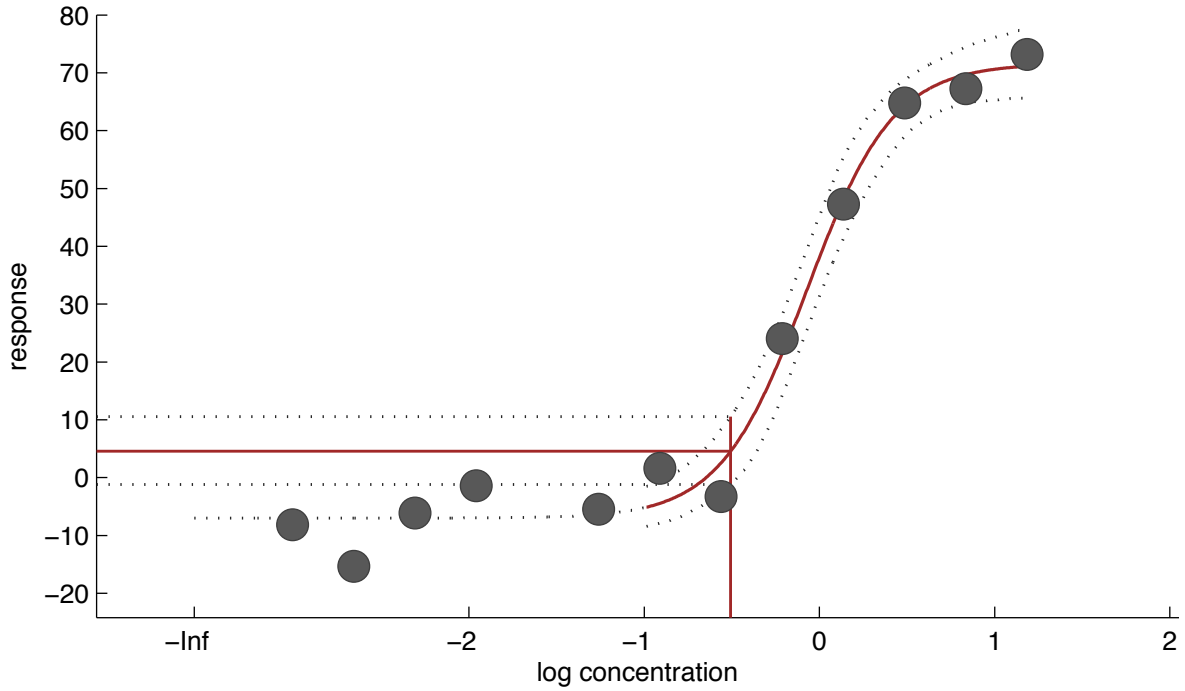
80
70
60
50
40
30
20
10
0
−10
−20
response
−Inf
−2
−1
0
1
2
log concentration

Figure 2a.

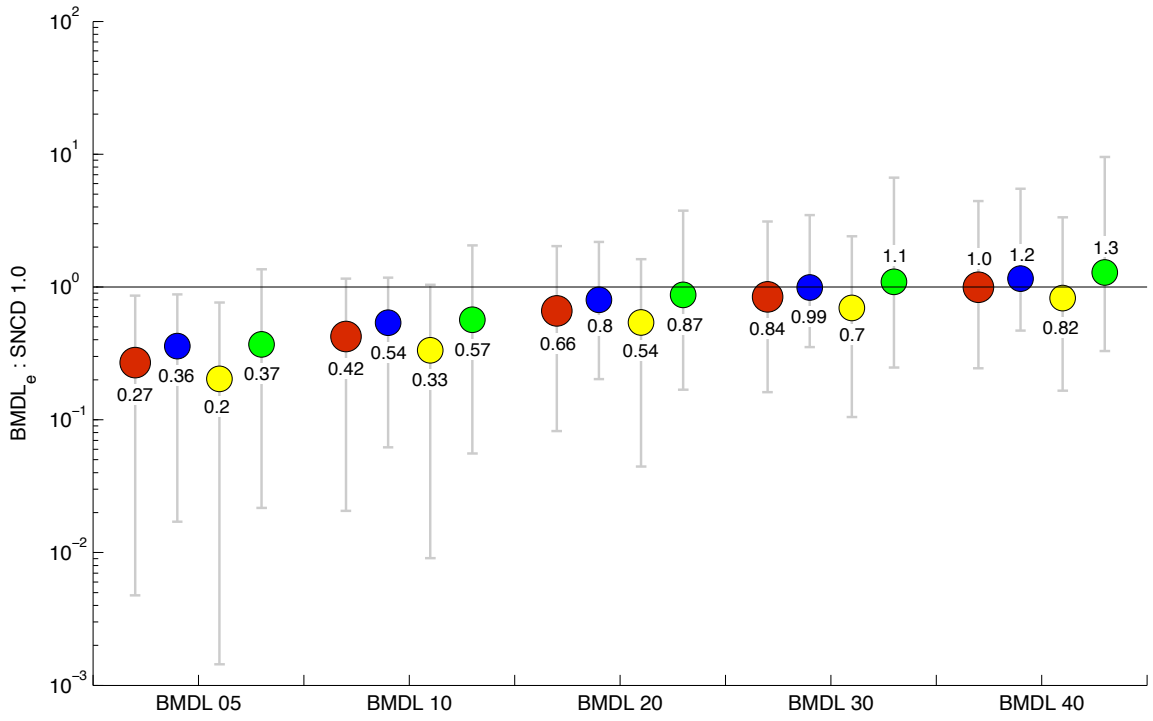
10^2
10^1
10^0
10^{-1}
10^{-2}
10^{-3}
$BMDL_e$: SNCD 1.0
0.27
0.36
0.2
0.37
0.42
0.54
0.33
0.57
0.66
0.8
0.54
0.87
0.84
0.99
0.7
1.1
1.0
1.2
0.82
1.3
BMDL 05
BMDL 10
BMDL 20
BMDL 30
BMDL 40

Figure 2b.

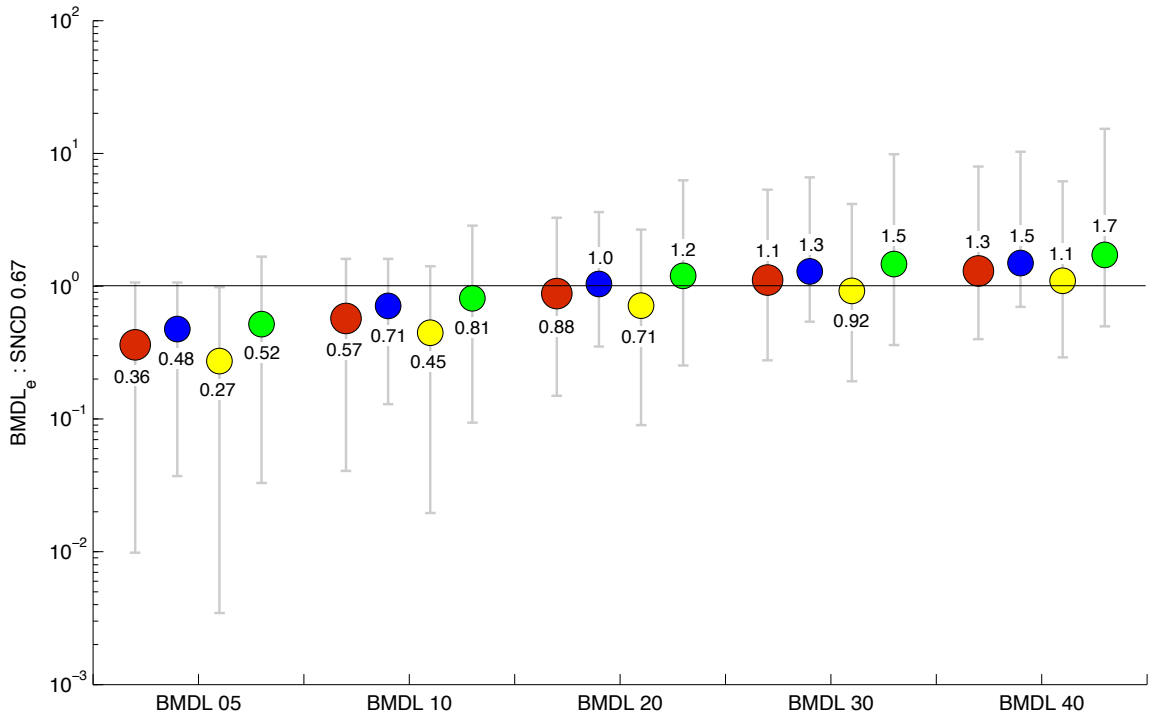
10^2
10^1
10^0
10^{-1}
10^{-2}
10^{-3}
$BMDL_e$: SNCD 0.67
0.36
0.48
0.27
0.52
0.57
0.71
0.45
0.81
0.88
1.0
0.71
1.2
1.1
1.3
0.92
1.5
1.3
1.5
1.1
1.7
BMDL 05
BMDL 10
BMDL 20
BMDL 30
BMDL 40

Figure 2c.

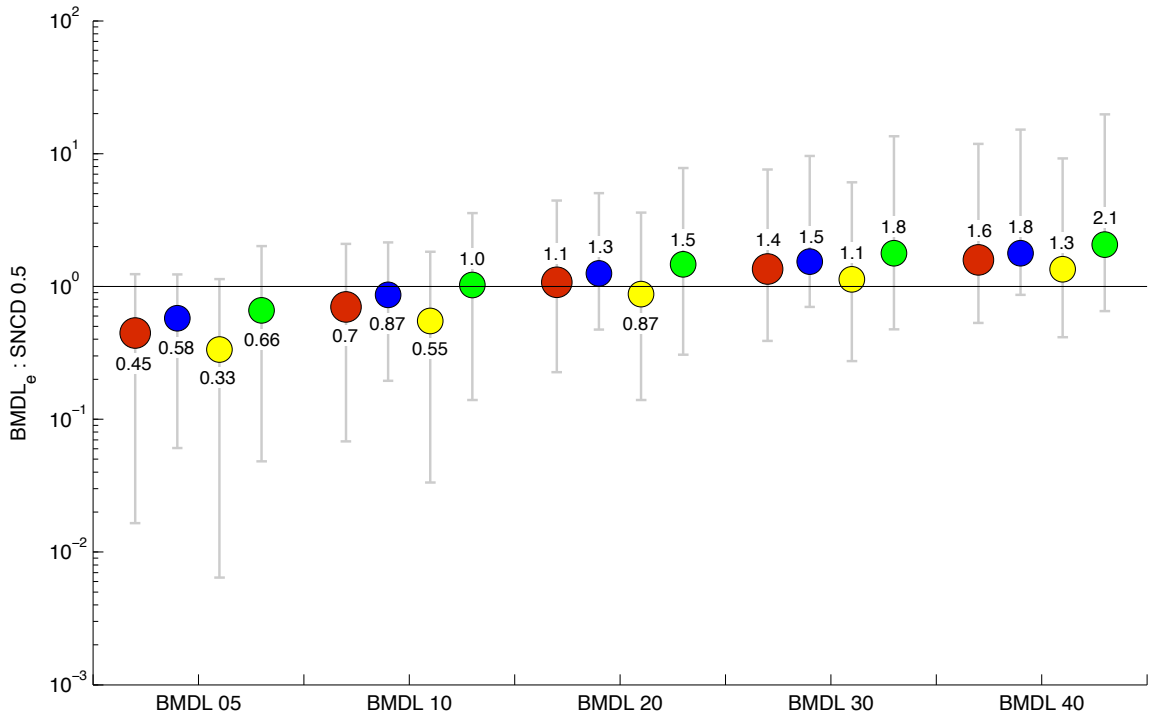
10^2
10^1
10^0
10^{-1}
10^{-2}
10^{-3}
$BMDL_e$: SNCD 0.5
0.45
0.58
0.33
0.66
0.7
0.87
0.55
1.0
1.1
1.3
0.87
1.5
1.4
1.5
1.1
1.8
1.6
1.8
1.3
2.1
BMDL 05
BMDL 10
BMDL 20
BMDL 30
BMDL 40

Figure 3.

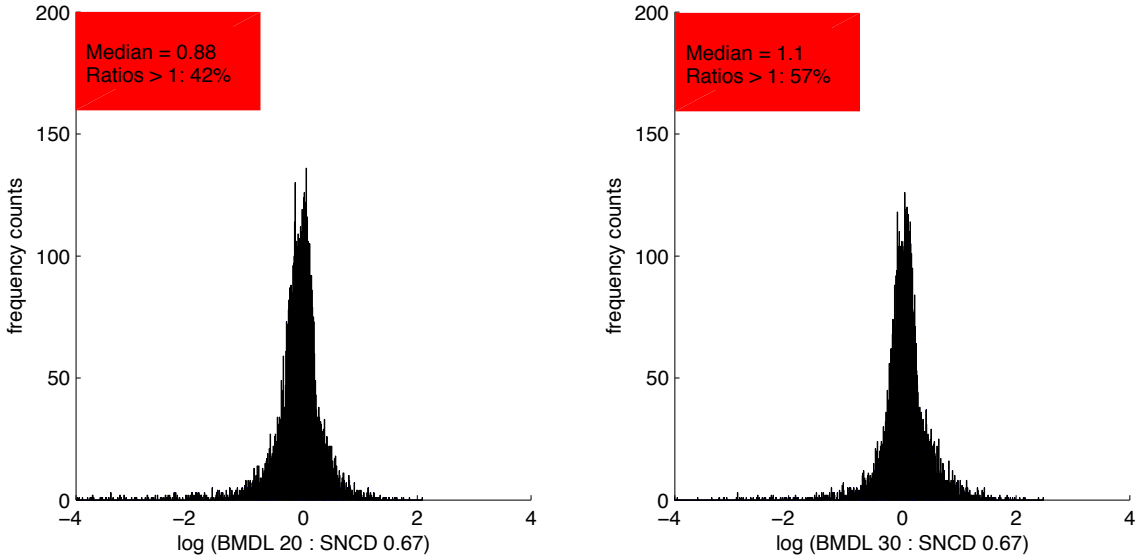
Median = 0.88
Ratios > 1: 42%
frequency counts
log (BMDL 20 : SNCD 0.67)
Median = 1.1
Ratios > 1: 57%
frequency counts
log (BMDL 30 : SNCD 0.67)

Figure 4a.

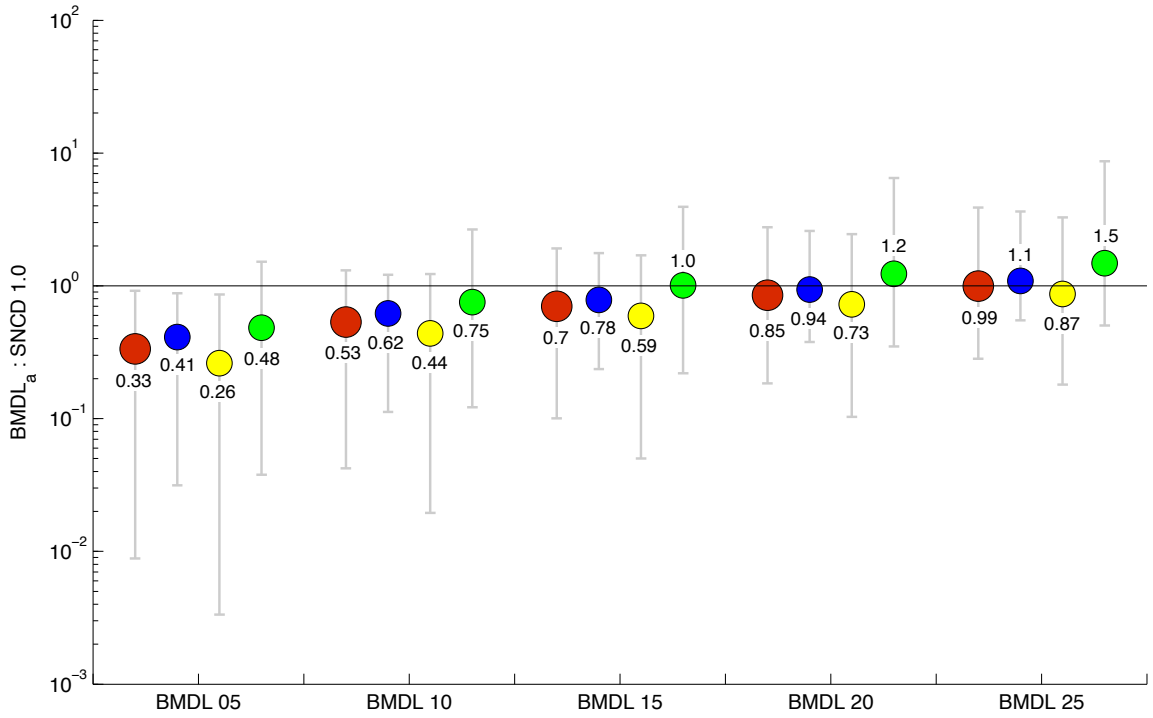
10^2
10^1
10^0
10^{-1}
10^{-2}
10^{-3}
$BMDL_a$: SNCD 1.0
0.33
0.41
0.26
0.48
0.53
0.62
0.44
0.75
0.7
0.78
0.59
1.0
0.85
0.94
0.73
1.2
0.99
1.1
0.87
1.5
BMDL 05
BMDL 10
BMDL 15
BMDL 20
BMDL 25

Figure 4b.

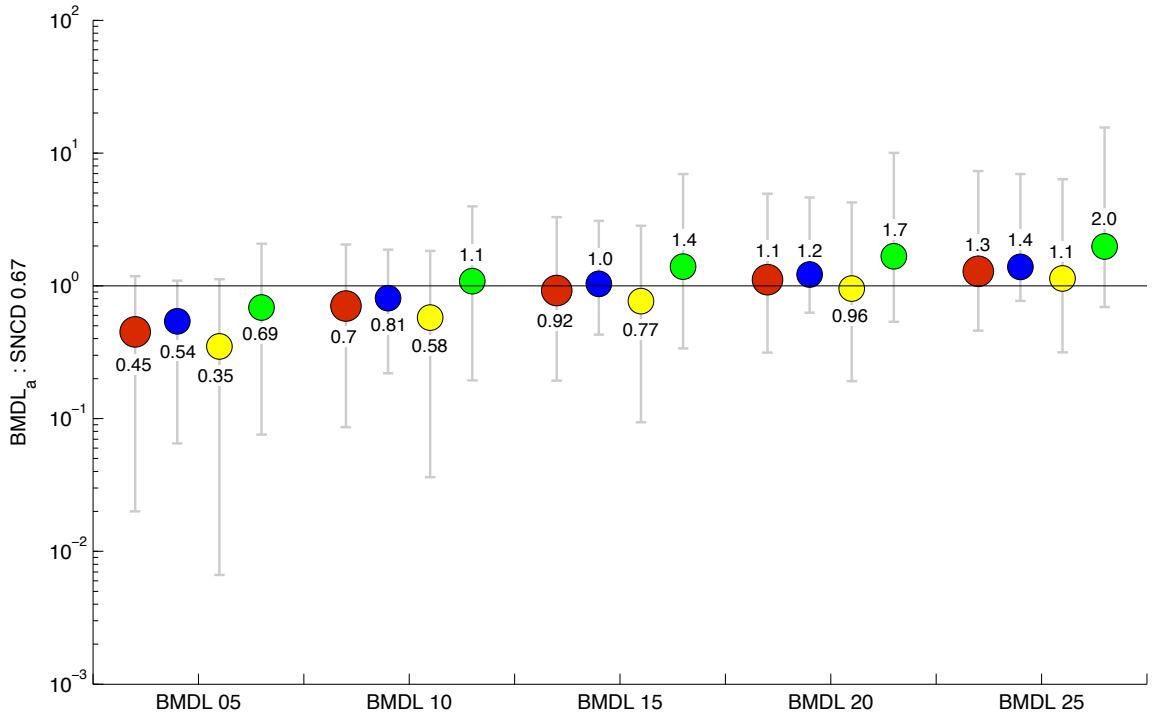
10^2
10^1
10^0
10^{-1}
10^{-2}
10^{-3}
$BMDL_a$: SNCD 0.67
0.45
0.54
0.35
0.69
0.7
0.81
0.58
1.1
0.92
1.0
0.77
1.4
1.1
1.2
0.96
1.7
1.3
1.4
1.1
2.0
BMDL 05
BMDL 10
BMDL 15
BMDL 20
BMDL 25

Figure 4c.

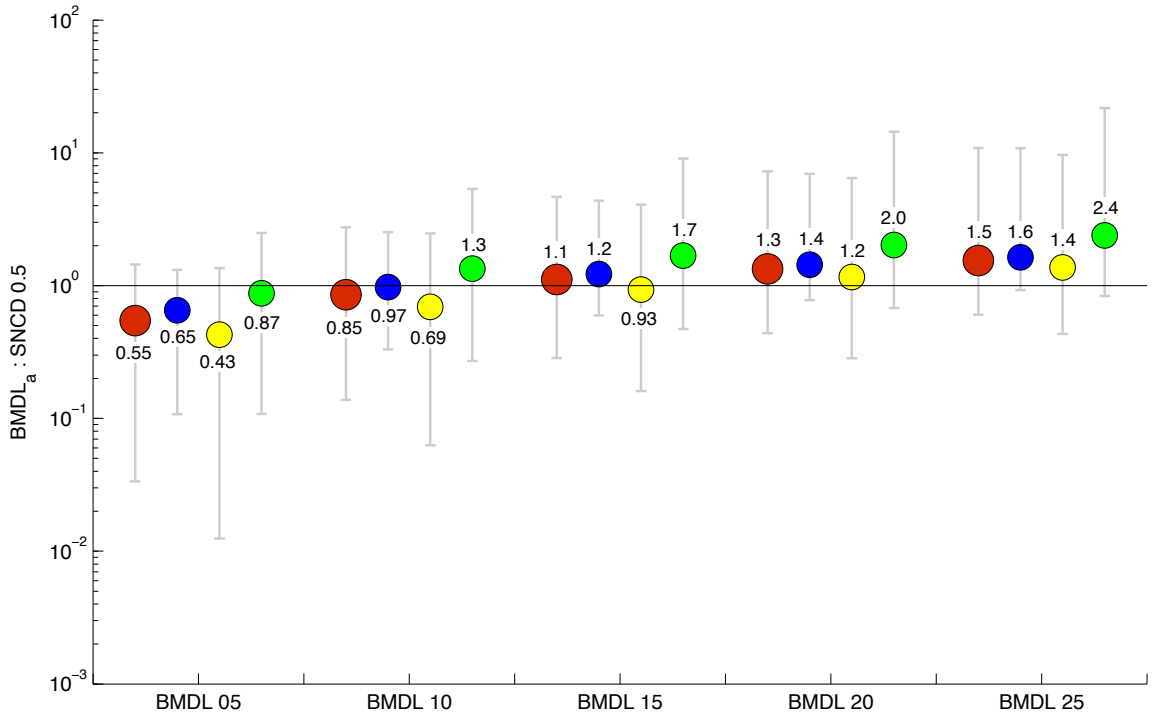
10^2
10^1
10^0
10^{-1}
10^{-2}
10^{-3}
$BMDL_a$: SNCD 0.5
0.55
0.65
0.43
0.87
0.85
0.97
0.69
1.3
1.1
1.2
0.93
1.7
1.3
1.4
1.2
2.0
1.5
1.6
1.4
2.4
BMDL 05
BMDL 10
BMDL 15
BMDL 20
BMDL 25

Figure 5.

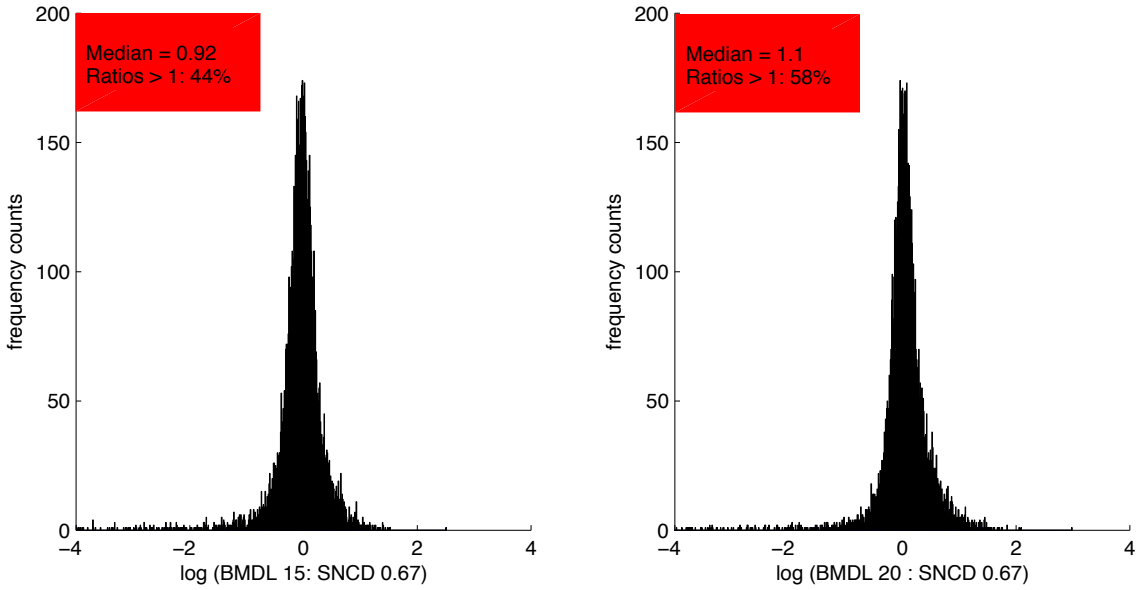
Median = 0.92
Ratios > 1: 44%
frequency counts
log (BMDL 15: SNCD 0.67)
Median = 1.1
Ratios > 1: 58%
frequency counts
log (BMDL 20 : SNCD 0.67)

Figure 6.

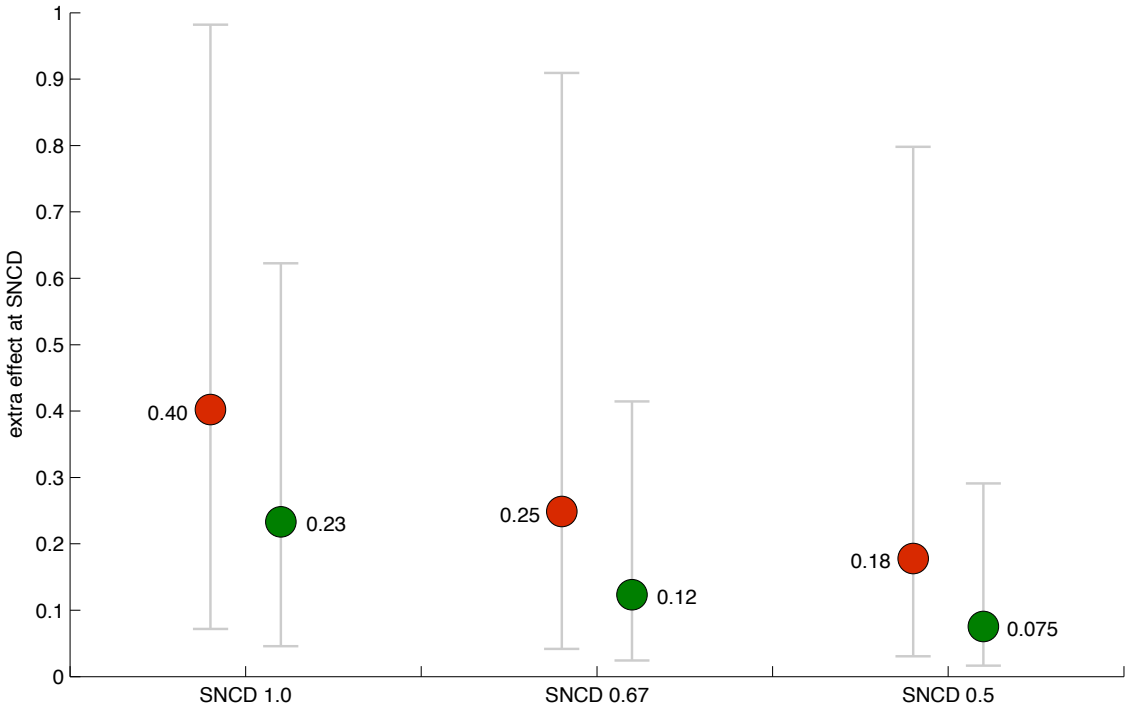
extra effect at SNCD
1
0.9
0.8
0.7
0.6
0.5
0.4
0.3
0.2
0.1
0
0.40
0.23
0.25
0.12
0.18
0.075
SNCD 1.0
SNCD 0.67
SNCD 0.5

Figure 7.

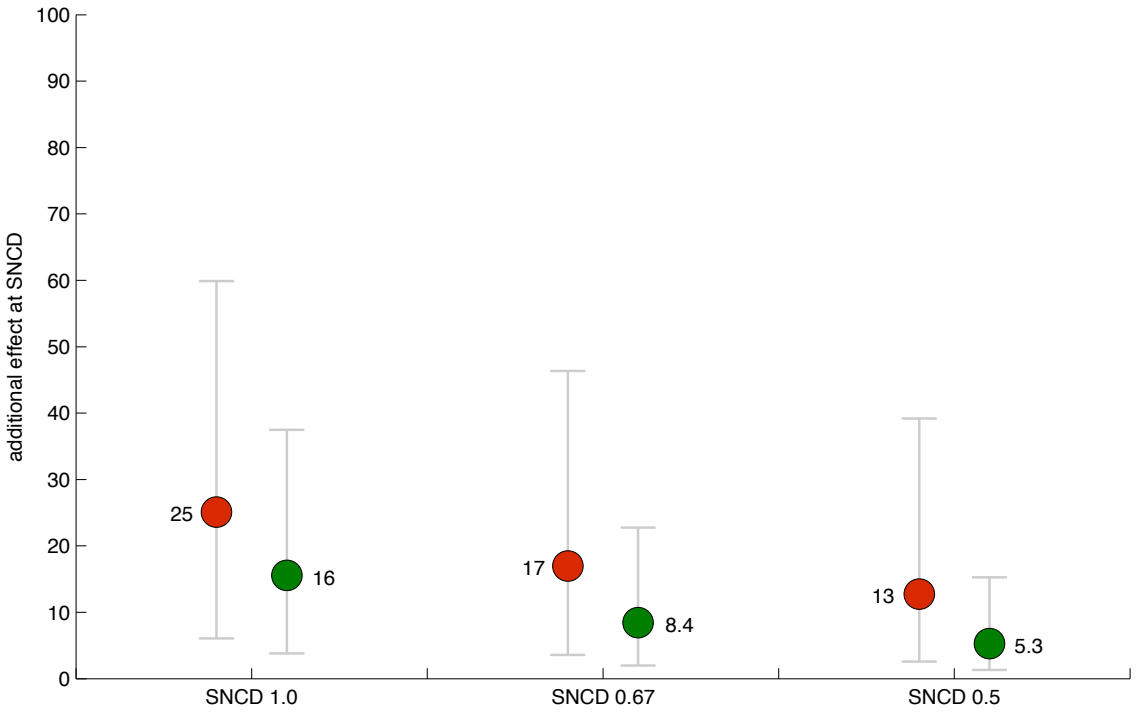
100
90
80
70
60
50
40
30
20
10
0
additional effect at SNCD
25
16
17
8.4
13
5.3
SNCD 1.0
SNCD 0.67
SNCD 0.5